Diamond & Related Materials 18 (2009) 82–87

Contents lists available at ScienceDirect

Diamond & Related Materials

journal homepage: www.elsevier.com/locate/diamond

Fluorescence quenching effects of nanocrystalline diamond surfaces

John J. Sakon [a], Guilhem J. Ribeill [a], Jacob M. Garguilo [a], James Perkins [a], Keith R. Weninger [a,*], Robert J. Nemanich [b]

[a] Department of Physics, North Carolina State University, Raleigh, NC 27695-8202, USA
[b] Department of Physics, Arizona State University, Tempe, AZ 85287-1504, USA

ARTICLE INFO

Article history:
Received 1 May 2008
Received in revised form 17 October 2008
Accepted 17 October 2008
Available online 5 November 2008

Keywords:
Nanocrystalline
Diamond film
Biocompatibility
Optical properties

ABSTRACT

Undoped diamond has conductive properties when terminated by hydrogen and exposed to air or aqueous solution. Here, it is shown that nanocrystalline diamond, fabricated with hydrogen termination and deposited on quartz substrates using chemical vapor deposition, significantly quenched the fluorescence of adsorbed, dye-labeled fibrinogen protein in aqueous solutions at near neutral pH. Smaller levels of quenching were observed from oxygen terminated NCD surfaces. We suggest that these near-surface fluorescence quenching effects may arise from surface conductance effects in hydrogen terminated NCD. It is also shown that despite bulk quenching effects, single molecules of fibrinogen could be imaged on nanocrystalline diamond surfaces using epi-fluorescence techniques.

1. Introduction

Undoped diamond is generally considered to be a very good insulator. However, an intriguing feature of thin films of undoped diamond grown by plasma-enhanced chemical vapor deposition (PECVD) is their p-type surface conductivity when they are terminated by hydrogen and exposed to air [1]. This phenomenon led to a number of models in an attempt to explain the conductive effect. It was initially thought that hydrogen neutralization of traps in the films lowered the resistivity of the diamond surface [1] or that the surface layer was oxidized by adsorbed gases [2]. It is now widely accepted that a surface transfer doping mechanism is at work, either through the formation of an electron sink by an H_2/H+ redox reaction in an adsorbed water layer [3,4] or possibly an O_2 couple similarly promoting surface transfer doping in the presence of adsorbed water [3,5,6].

Recently, Chakrapani et al. [5] have shown strong evidence that the conductivity of hydrogen (H)-terminated diamond is a result of charge transfer from the surface to an O_2 redox couple in an adjoining water phase. Their experiments involved titrating single crystal H-terminated diamond powder in aqueous solution at various initial pHs and subsequently measuring the changes in pH and dissolved oxygen concentration. They determined that the electron transfer at various pH values was consistent with the electrochemical redox reaction involving dissolved oxygen in water in contact with the H-terminated diamond surface [3,5,6].

A well known property of surface conductors is the quenching of emission from adsorbed fluorescent molecules [7,8]. Here, we present evidence of fluorescence quenching by H-terminated nanocrystalline diamond (NCD) surfaces in aqueous solutions at physiological pH (7.4). This research involved adsorbing human fibrinogen protein to H-terminated NCD surfaces that were deposited on quartz microscope slides using PECVD. In the first experiment, fibrinogen was labeled with amine-reactive Alexa-555 fluorescent dye, added to flow channels over various sample surfaces and washed to ensure only adhering protein remained. Fluorescence imaging was used to measure emission levels from protein adsorbed to the surface. In the second experiment fibrinogen labeled with radioactive I-125 was flowed onto the same surfaces using the same methodologies as the fluorescence experiment and radioactivity was measured to determine the amount of protein that adhered.

The optical tests showed significantly less fluorescence from H-terminated NCD surfaces exposed to dye-labeled fibrinogen than control quartz samples when equal amounts of the protein – at three different concentrations – were added to each surface. The fluorescence levels of protein bound on NCD were more akin to that of polyethylene glycol (PEG) coated quartz, which is known to minimally adsorb protein [9–11]. Fluorescence from dye-labeled fibrinogen exposed to oxygen (O)-terminated NCD surfaces was less than the bare quartz controls, but was significantly higher than the H-terminated NCD.

The radioactivity tests determined that radio-labeled fibrinogen adsorbed to all the surfaces, H-terminated NCD, O-terminated NCD and bare quartz, in nearly equal amounts when exposed to the protein under constant times and concentrations. The binding of protein to PEG-coated quartz remained relatively low compared to the other surfaces in the radiation study.

* Corresponding author.
E-mail address: keith_weninger@ncsu.edu (K.R. Weninger).

0925-9635/$ – see front matter © 2008 Elsevier B.V. All rights reserved.
doi:10.1016/j.diamond.2008.10.028

These results, in which fluorescence of equal amounts of adsorbed protein was less on H-terminated NCD than bare quartz, indicate fluorescence quenching occurs at the surface of the H-terminated NCD sample. Fluorescence quenching is commonly a result of electromagnetic coupling between the fluorescing molecule and a conductive surface. This effect allows strong energy transfer from the molecule to the surface and a subsequent loss in fluorescent intensity [7,8]. We attribute this quenching to the conductance of a positive space charge layer on the NCD surface that forms from the electrochemical redox reaction outlined above. The intermediate quenching from the oxygen surface suggests that the oxygenation process applied to the initially H-terminated surface was incomplete.

Additional tests found that, despite the fluorescence quenching effects at bulk protein concentrations, a few single molecules of dye-labeled fibrinogen could be imaged on the NCD surface at higher illumination intensities. Possible explanations for this effect are discussed.

2. Materials and methods

The initial substrates for all experiments were 1″×3″ quartz microscope slides (G. Finkenbeiner, Inc., Waltham, MA). Prior to any surface treatment, five 1 mm diameter holes were drilled on each 3″ side of each slide. After drilling, slides were cleaned with a sequence of 15-minute incubations in a bath sonicator in Alconox (White Plains, NY) detergent/water, acetone, ethanol, 1 M potassium hydroxide and de-ionized water in that order. Uncoated slides, thoroughly cleaned by this sequence, were used as the control quartz substrates in the experiments.

NCD thin films were deposited onto quartz slides using microwave plasma enhanced chemical vapor deposition (MPCVD). Careful optimization of the growth parameters was required to achieve NCD films with sufficiently low optical absorbance and auto-fluorescence to allow the measurements reported here. The MPCVD reactor used for deposition was a 1500-W ASTeX IPX3750 microwave-assisted CVD system with an RF induction-heated graphite susceptor. Prior to deposition, the clean quartz substrates were ultrasonically pretreated in slurry consisting of 0.15 g diamond powder (<1 μm particle size, Alfa Aesar) and 0.15 g titanium powder (−325 mesh/<44 μm particle size, Alfa Aesar) in 15 mL of methanol for 15 min. The substrates were then rinsed in acetone and methanol for 5 min and loaded into the deposition system. The process gases for growth of hydrogen terminated NCD were zero-grade H_2 and CH_4. During film growth, laser reflectance interferometry (LRI) was used for in situ monitoring of the thickness of the diamond layer. NCD films were grown under flows of 180 sccm H_2 and 20 sccm CH_4, while growth conditions were a chamber pressure of 1.67 kPa, thermocouple temperature of 600 °C and microwave power of 900 W. These conditions were typically maintained for 90 min resulting in an approximate film thickness of 250 nm. The as-deposited films are terminated with a monolayer of hydrogen.

Oxygen-terminated NCD was also deposited on quartz slides via the method outlined by Maier et al. [12]. Briefly, the H-terminated NCD coated slides were annealed in vacuum at 665 °C for 30 min, boiled in 1:3 HNO_3:H_2SO_4 at 350 °C for 15 min and then rinsed with deionized water. All experiments using O-terminated or H-terminated NCD were conducted within 10 days of the initial preparation of the diamond films.

For comparison with the NCD films, PEG monolayers were formed on quartz slides by first coating the slides with an amino-silane layer by soaking in a mixture of 1% (v/v) 3-Aminopropyl triethoxysilane (Sigma-Aldrich, St. Louis) in acetone for 5 min. Next, 100 mg/mL mPEG-Succinimidyl Propionate (Nektar, San Carlos, CA) in a 0.1 M sodium bicarbonate solution was incubated between the quartz slide and a similarly amino-silane modified glass coverslip for 1.5 h in the dark. Unbound PEG was washed away by extensive rinsing with de-ionized water.

After growth, room temperature Raman spectra of the NCD films were recorded. Visible Raman measurements were completed with an ISA U-1000 scanning double monochromator using the 514.5 nm line of an argon ion laser as the excitation source. Ultraviolet Raman measurements were excited with the 244 nm line of a frequency-doubled Coherent Inc. Innova 300 FreD argon ion laser, the scattered light was collected in a backscattering geometry and imaged onto the entrance slit of a SPEX 1877 TripleMate spectrometer. Atomic force microscopy (AFM) was performed on the films using an Autoprobe CPR Microscope (Park Scientific) in contact mode with Si_3N_4 tips.

Type 1 human plasma fibrinogen was purchased from Sigma-Aldrich. Alexa Fluor 555 carboxylic acid, succinimidyl ester (Invitrogen, Carlsbad, CA) was dissolved in 5 μL pure dimethylsulfoxide and mixed at 5 M dye:1 M protein overnight in 0.1 M $NaHCO_3$ to form amine linkages with fibrinogen. Conjugated protein was separated from free dye by passing the reaction over a PD-10 gel filtration column (GE Biosciences, Piscataway, NJ) equilibrated with 25 mM Phosphate buffer (pH 7.4), 150 mM NaCl (PBS). UV–VIS absorption spectrophotometric analysis showed ~1:1 molar concentrations of dye conjugated to fibrinogen (i.e. ~1 dye molecule per protein).

To label fibrinogen with radioactive I-125, 120 μL of 0.4 mg/mL protein was added to a pre-coated IODO-GEN reaction tube (Pierce, #28601) along with .25 mCi of Iodine-125 Radionuclide (PerkinElmer). After allowing this reaction to proceed for 15 min on a rocker, unbound iodine was removed with a 0.5 mL desalting column (Pierce, #89882) run in PBS. Protein concentration was measured by UV–VIS absorption after desalt.

For both the fluorescence and radiation tests, flow chambers holding approximately 25 μL were constructed on the substrates by isolating opposing pre-drilled holes with thin strips of double-sided tape (3M, St. Paul, Minnesota) and placing a PEG-coated no. 1.5 coverslip over the slide. The ends of these chambers were sealed using epoxy glue (Huntsman, Los Angeles, CA); to prevent contamination the glue was allowed to set for at least 1 h. No fluorescent contamination was observed from the tape and glue used in the flow chambers in control observations without introduction of dye-labeled protein. The liquid sample/buffer could be exchanged through each channel by micropipetting through the pre-drilled holes at the end of these chambers.

The channels were filled with 100 μL of protein solution at the desired concentration, allowed to incubate for 5 min and then flushed with 200 μL of PBS. Additional rinsing did not change the results. For the fluorescence tests, the time the protein was allowed to incubate in the channel (<1 h) and the delay between incubation and data acquisition (ranging from 1 min to 48 h) had little effect on the measured results. Concentrations used were 10, 50 and 100 nM fibrinogen for bulk studies and 50 pM for single molecule measurements.

To image the channels, an IX71 inverted microscope (Olympus, Melville, NY) was used with an Olympus UPlanSApo 60× water immersion lens. Excitatory light from a 532 nm laser (Swutech, Shanghai, China) was directed to the sample in epi-illumination mode through a Z532–633 dual band-pass dichroic mirror (Chroma Technology, Rockingham, VT) below the objective. The intensity at the sample for bulk fluorescence measurements was 1 mW, while single molecule data was taken with 10 mW illumination. Bulk fluorescence measurements utilized a 550 nM long pass filter (Chroma) to separate fluorescence emission from laser light. For single molecule measurements, a Cy3/Cy5 emission filter (part # 51700m , Chroma) blocked the scattered laser light. 100 frame movies at a frame rate of 10 frames/s were acquired through a custom program using a Cascade 512B CCD camera (Photometrics, Tuscon, AZ). Analysis of the data was performed with custom MATLAB programs: for bulk measurements, the average intensity over the entire frame was recorded for 100 frames (100 ms exposure) whereas for single molecule experiments, intensity timecourses were generated for intensity peaks found in the frame.

Radioactivity of protein bound to substrates was measured by taping the substrates to film (Kodak BioMax MR) for 8–48 h followed by standard development (Konica Minolta SRX-101A). The large time range is indicative of the loss of radioactivity of the I-125 (half life=60.14 days)

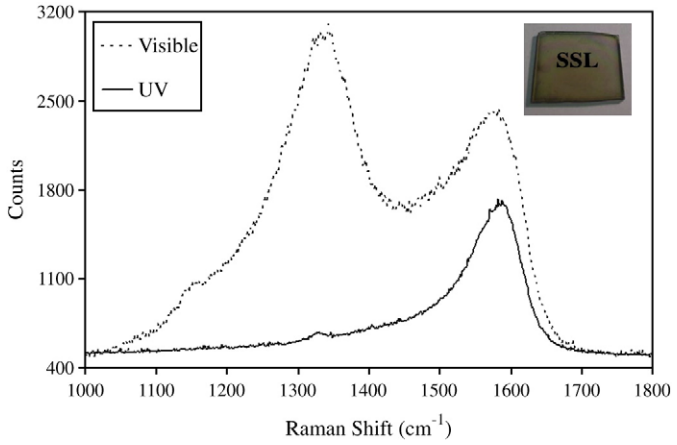

Fig. 1. Raman spectroscopy of a typical hydrogen (H)-terminated nanocrystalline diamond (NCD) film deposited on quartz. The visible spectrum's main peaks consist of the D-band peak at ~1340 cm^{-1} and the G-band peak at ~1556 cm^{-1}, which are associated with sp^2 bonding in carbon. A small shoulder at 1140 cm^{-1} is present. This has been attributed to sp^2-bonded carbon, NCD, or transpolyacetylene segments at grain boundaries and surfaces. The UV measurements show a large peak at ~1556 cm^{-1} associated with sp^2 bonding and a small diamond peak located at 1334 cm^{-1}. The transparency of these NCD films deposited on quartz substrates is evident in the image of a typical sample displayed in the inset.

sample over the course of multiple experiments. Exposure time scales did not affect the data as it is presented relative to (quartz) controls present at each experiment and therefore is not an absolute value. Film images were digitally scanned and analyzed using ImageJ (NIH). Darkness levels – indicative of exposure to radiation by protein absorbed to the slides – were measured by subtracting backgrounds taken in adjacent swaths of film not in direct contact with the flow channel areas of the slides.

Contact angle was measured using GIMP software (www.gimp.org) to analyze digital photographs of de-ionized water droplets on the surfaces.

3. Results and discussion

Raman spectroscopy of a NCD film on a quartz substrate is shown in Fig. 1 and is representative of typical nano-structured diamond. Visible Raman spectroscopy of carbon-based materials is dominated by scattering from sp^2 hybrids as the sensitivity to these contributions is ~100 times that of diamond [13]. There are several identifiable peaks in the spectrum: the D-band peak at ~1340 cm^{-1}, the G-band peak at ~1556 cm^{-1} and a shoulder at 1140 cm^{-1}. The G (graphite) mode is associated with stretching vibrations of any pair of sp^2 sites while the D (disorder) mode corresponds to a breathing mode of sp^2 aromatic rings. The D mode is only active when disorder is present in the film; it is forbidden in perfectly crystalline graphite. The 1140 cm^{-1} peak has been attributed to sp^2-bonded carbon, NCD, or transpolyacetylene segments at grain boundaries and surfaces [14–16]. The UV measurements show a large peak at ~1556 cm^{-1} associated with sp^2 bonding and a small diamond peak located at 1334 cm^{-1}. With UV excitation, the ~ 1332 cm^{-1} peak associated with diamond crystalline domains becomes more evident. This is due to two effects: 1) the relative intensity of the ~ 1350 cm^{-1} D-peak decreases in the UV, and 2) the relative intensity of the diamond crystalline peak is enhanced due to resonance effects [15]. Thus, for nanocrystalline diamond films, UV Raman scattering is often employed to detect the diamond feature [14]. The deposition conditions of the films used in this study were optimized to achieve the lowest photoluminescence background in the UV-visible wavelength region. The UV Raman of the diamond peak for these samples was somewhat reduced relative to the sp^2 related features, but the films are still largely diamond as evidenced by their transparency (Fig. 1 inset). NCD films deposited on silicon wafers under the same conditions as the films in this study have nearly identical Raman spectra while Near Edge X-ray Absorption Fine Structure (NEXAFS) measurements of these films indicate they are composed of approximately 14% sp^2 bonding, presumably localized to the grain boundaries of the film (data not shown). The AFM measurements are presented in Fig. 2 and show a polycrystalline surface having a relatively smooth character with an approximate RMS roughness of 4.1 nm. This value, along with the absence of large hillocks in the AFM indicates that the titanium and diamond particles in the pre-treatment slurry were removed in the subsequent washing. Furthermore, any residue of the particles remaining on the surface via fracturing during sonication will have been overgrown by the diamond and would not be exposed to the fibrinogen. The surface morphology indicates the presence of many small grains and grain boundaries, typical of NCD.

The results of the fluorescently tagged protein binding experiments, in which Alexa-555-labeled fibrinogen was exposed to NCD surfaces and measured on a fluorescence microscope, are presented in Fig. 3. These experiments were repeated for at least three identically grown NCD samples, and data was obtained from at least 5 locations on each sample and averaged to give the resulting values. At each concentration tested, quartz substrates showed significantly higher fluorescence intensity than PEG and H-terminated NCD. The PEG monolayers showed the lowest fluorescence at all concentrations, slightly lower than NCD. Oxygen-terminated NCD was also tested for comparison and showed fluorescence intensity approximately midway between quartz and H-terminated NCD.

Fig. 4 displays the results of the I-125 radio-labeled protein binding experiments, which involved the adsorption of radioactive iodine-labeled fibrinogen to NCD surfaces and subsequent measurements using photographic film. The bars show the average of at least three experiments. Surprisingly, in dramatic contrast to the fluorescence measurements, H-terminated NCD bound similar amounts of fibrinogen as control quartz samples at all concentrations tested. Further, O-terminated NCD bound the radioactive fibrinogen about the same as quartz despite showing lower signal than bare quartz in the

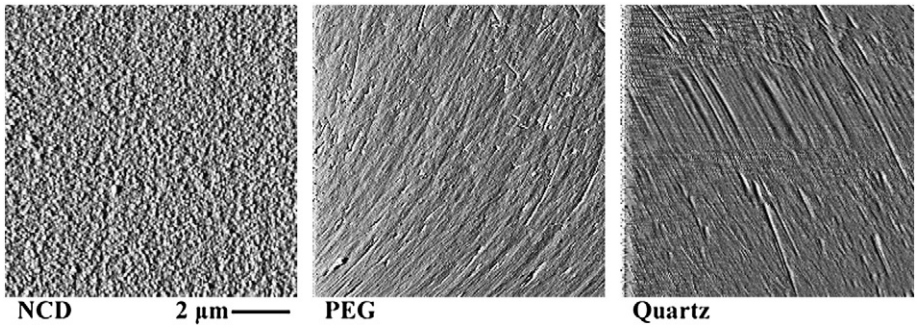

Fig. 2. AFM phase imaging of an NCD film (left), a PEG-coated quartz slide (center) and a bare quartz slide (right) at fields of view of 10 μm. The NCD possesses a finely grained structure with many grain boundaries and has an RMS roughness of 4.1 nm. The PEG coating and quartz slide have RMS roughness values of 1.6 nm and 7.5 nm, respectively.

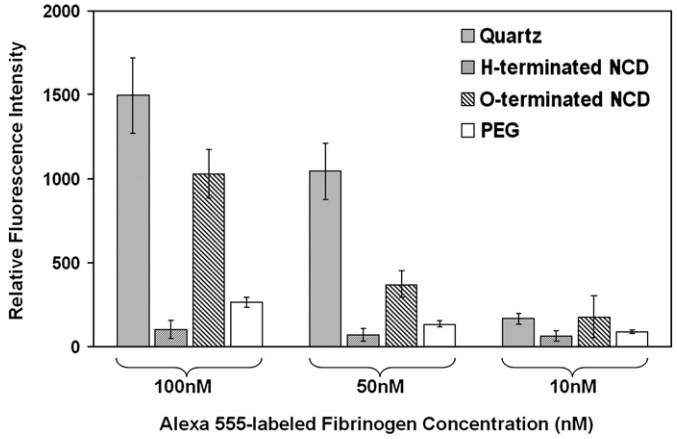

Fig. 3. The fluorescence of adsorbed fibrinogen on quartz, H-terminated NCD, oxygen (O)-terminated NCD and PEG monolayers measured at three different protein concentrations: 10 nM, 50 nM, and 100 nM. Fluorescently tagged fibrinogen solutions were introduced to the surfaces for 5 min through sealed channels. After exposure, the surfaces were flushed with PBS Buffer and the fluorescent signal was recorded. The background for each sample was then subtracted to give the resultant fibrinogen signal. This measurement was repeated for at least 3 samples of each type, and for 5 or more data points on each sample. These values were then averaged to give the above data. The results show large fluorescence signal on quartz surfaces with significantly lower signal occurring on NCD and PEG surfaces. Error bars reflect standard deviation of at least 5 values taken from different regions on 3 different samples.

fluorescence tests. Similar to the fluorescence experiments, PEG bound less protein than quartz. Experiments done with 10 nM radio-labeled fibrinogen resulted in adsorption that was too low to quantitatively compare using this methodology. Nonetheless, the same qualitative trends were evident at 10 nM: H-terminated and O-terminated NCD bound similar amounts of protein as bare quartz, which in turn bound more protein than PEG (data not shown).

These experiments display a clear discrepancy. Radio-labeled protein measurements indicate similar adsorption of fibrinogen on H-terminated NCD, O-terminated NCD and untreated quartz surfaces, whereas fluorescence emission from dye-labeled fibrinogen is dramatically lower on H-terminated NCD compared to quartz or O-terminated NCD. Adsorption to PEG surfaces was the lowest as indicated by both radiation and fluorescence tests.

This discrepancy can be resolved if proximity to the H-terminated NCD film quenches the fluorescence of the dye-labeled protein [8]. As detailed above, H-terminated NCD has been shown to have significant conductive properties [1–6]. While it is common that surfaces of conductive materials have fluorescence quenching effects, it is an intriguing result to find that H-terminated NCD quenches fluorescence at a pH as high as 7.4. Chakrapani et al. [5] found that the electron transfer at various pHs was consistent with that of an electrochemical redox reaction involving dissolved oxygen in water in contact with the H-terminated diamond surface [3,5,6]. At pH 7.4 and atmospheric p_{O_2} of .21 bar, the Nernst equation predicts the electrochemical potential of electrons for this redox couple to be −5.22 eV. Considering the electron affinity of H-terminated diamond in contact with water and the diamond band gap [5], electrons in this redox reaction are at or just above the expected valence energies. When electrons have this requisite energy to cross the band gap, holes are created on the diamond surface and are responsible for the conductance effect seen in H-terminated diamond.

Other experiments by Chakrapani et al. [5] also support conductivity at pH 7.4. Zeta potentials were measured at various pHs to confirm the direction of electron transfer between single crystal H-terminated diamond and water. At pH=6, the zeta potential was clearly positive (~15 to 20 mV). At pH~7.7, the zeta potential was slightly negative (~0 to −5 mV) [5]. From these measurements, it is clear that crossover between positive and negative zeta potential must occur between pH 6 and 7.7, with the precise value of the crossover having implications for conductance at the physiological pH used in our studies.

It should be noted that when H-terminated diamond was added to aqueous solutions at starting pHs between 7 and 10, Chakrapani et al. [5] found a significant negative change in pH in this starting range. A drop in pH, i.e. higher hydronium ion concentration, is indicative of retention of surface holes even at these initially high pHs. Therefore, even at higher pHs, it appears a certain number of holes are still present on the surface.

Providing additional evidence of this point, Foord et al. [6] measured the conductivity of CVD H-terminated diamond at various pHs in solution using gold contacts that were attached to the surface prior to deposition. Their results, which show a marked decrease in conductivity as the pH of the solution in contact with the diamond surface was raised, correlate with the redox reaction confirmed in Chakrapani et al. [5]. These measurements found significant conductivity at pHs in the 7–8 range — albeit a factor of two less in conductivity than the surface in contact with a solution at pH 1. These results further support the fluorescence quenching effect seen in our experiments as deriving from the conductivity of the H-terminated NCD surfaces.

A complication in our experiments is the residual quenching seen in NCD terminated with oxygen. Fluorescence of dye-labeled protein on O-terminated NCD was lower than quartz – albeit much higher than H-terminated NCD (Fig. 3) – despite nearly equal protein binding as determined using radio-labeled fibrinogen (Fig. 4). Oxidized diamond in contact with water has a band gap too large to allow the valence band to be near the electrochemical potential of electrons predicted by the Nernst equation [17]. It is possible that our protocol for forming O-termination on initially H-terminated NCD surfaces is imperfect and allows a limited amount of hydrogen to remain on the samples. Maier et al. [12] found that the acid treatment does not completely remove chemisorbed hydrogen from the sample surface during passivation. Residual hydrogen could lead to partial fluorescence quenching by the O-terminated surfaces. At this time we cannot completely rule out the possibility that defective states or impurities in the bulk of the NCD films contribute to quenching. On the other hand, the different quenching properties of the O and H terminated NCD likely arise from surface effects because the O-terminated NCD was prepared by modifying the surface of an initially H-terminated NCD.

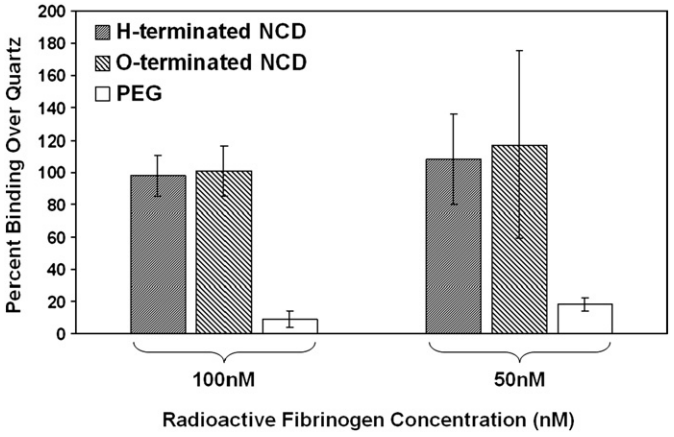

Fig. 4. Two different concentrations of I-125 radioactively-labeled fibrinogen were flowed over quartz slides with surface-deposited, H-terminated NCD, O-terminated NCD or Polyethylene Glycol (PEG) and pressed against a piece of film for a number of hours. Swaths of film, which darken with respect to the amount of radiation emitting from the sample, indicate adsorption of the radioactive protein. Results are shown as percent binding in comparison to identical tests done with quartz controls. The bars show the average of at least 3 experiments while the error bars reflect standard deviation of at least 5 values taken from different regions on each sample.

A further concern in our experiments is the possible oxidation of H-terminated diamond upon exposure to air. Fluorescence quenching was found to occur with NCD samples tested as short as 1 day and as long as several months after deposition (data not shown), indicating a robust resiliency of the quenching phenomena of these surfaces to exposure to air as well as our cleaning solutions. Surface characterization of the NCD surfaces used in our experiments by water contact angle measurements found angles of 64±12° and 9±3° for hydrogen and oxygen-terminated samples, respectively (data not shown). These are in line with previous results that show H-terminated NCD and hydrogen-terminated polycrystalline diamond deposited on silicon have water contact angles ~90° while oxidized polycrystalline diamond has an angle ~30° [18,19]. Adsorbed films can also affect contact angles. For the NCD samples used in our studies, the possibility remains that the contact angles are dominated by the exposed grain surfaces whereas the quenching may arise at the H-terminated grain boundaries within the interior of the NCD film. Regardless of the specific phenomena resulting in the low water contact angles of our samples, strong fluorescence quenching effects were observed from all of the H-terminated NCD surfaces used in our study.

The results of the radiation experiments, in which radio-labeled fibrinogen adsorbed to NCD surfaces more than quartz, question the usefulness of H-terminated NCD for blood-contacting device fabrication, in contrast to previous reports of low adhesion of biological substrates to NCD [20–23]. However, there are a number of experimental differences between these papers and this research. NCD was deposited on silicon [20,21,23] or steel [22] surfaces in these works as opposed to the quartz slides employed in our experiments. Further, most of these reports did not specify the fabricated surface termination of the NCD they used. Chong et al. [20] did use hydrogen-terminated diamond, but measured the adherence of cell adhesion to these surfaces instead of protein. Cell membrane proteins have functions distinct from fibrinogen and are therefore expected to have different binding properties.

Okroj et al. [22] raise one interesting possibility relevant to the high protein binding in our experiments: the increased binding of blood-containing proteins to damaged NCD surfaces. While we do not believe bath sonication in the various solvents used in our cleaning method should significantly damage the NCD surface – in fact, the AFM images in Fig. 2 were taken after the surface was cleaned using this method – it remains a possibility that certain regions could be compromised and present nucleation sites for protein binding. Regardless, if such damage did exist, it did not affect the overall quenching result in any of our fluorescence experiments.

One way to probe for local heterogeneity in the NCD surface is to image fluorescence from single molecules of fibrinogen adsorbed from lower concentration solutions (50 pM) to the surface of NCD under stronger illumination (10 mW). Fig. 5 displays microscopy measurements in epi-illumination mode of a single fibrinogen-attached fluorophore as well-defined Gaussian peaks. Time traces of fluorophore intensity (Fig. 5) show quantized photobleaching in single steps down to background levels, which is a behavior characteristic of single molecules [24]. The signal to noise ratio was found to be 2.15:1 ($n=10$), as defined by:

$$\left[\overline{x_{on}}-\overline{x_{off}}\right]/\sqrt{\left(\sigma_{on}^{\ 2}+\sigma_{off}^{\ 2}\right)} \tag{3}$$

where $\overline{x_{on}}$ and $\overline{x_{off}}$ represent the average intensity values before (on) and after (off) bleach and σ_{on} and σ_{off} are the standard deviations of the signal in their respective states. The poor signal to noise ratio is in large part a result of the background fluorescence of the diamond, which could be improved by further work on growth conditions. The possibility of partial fluorescence quenching also exists (see discussion below). This background fluorescence, coupled with the modest absorption of diamond films at 532 nm (data not shown), forced the use of epi-fluorescence instead of the more common total internal reflection method for single molecule imaging [25].

The ability to resolve single molecules on NCD seems contradictory to the observed fluorescence quenching effects. One explanation is local variability in the NCD properties at the site of these individual molecules. Spatial variations in composition or structure of the surface layer might lead to local inconsistencies in quenching efficiency. Alternately, single molecule fluorescent emission can be attributed to the dye being located at a height in the z-direction above the NCD surface that takes it beyond the quenching distance. Fluorescence quenching on conductors has been shown to dominate at distances <5 nm from the surface [8]. However, at larger distances, peaking ~20 nm, fluorescence is no longer fully quenched and can even be enhanced [8,26,27]. AFM images of fibrinogen bound to both hydrophilic and hydrophobic silicon surfaces have shown the protein extending in the z-direction as high as 15 nm [28]. However, much of the protein remains closer to 5 nm in height [28]. Therefore, it is plausible that the majority of fluorescence from samples with large amounts of adsorbed dye labeled protein is either fully or partially quenched. Meanwhile, occasional molecules might extend far enough from the surface to avoid significant quenching depending on the orientation of the surface tethering since fibrinogen dimers are 50 nm long [29].

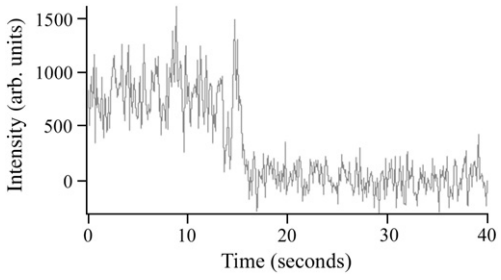

Fig. 5. A plot of intensity vs. time for a fluorophore adsorbed onto H-terminated NCD at a concentration of 50 pM and excited with a 532 nm laser at 10 mW. The single-step photobleach of the fluorophore after approximately 15 s is indicative of single molecule fluorescence microscopy (the intensity is measured in relative units). The signal to noise of the event is approximately 2.15:1.

4. Summary

H-terminated NCD, deposited on quartz substrates with chemical vapor deposition, has shown strong fluorescence quenching effects at physiological pH. This fluorescence quenching may arise from the conductive properties of H-terminated NCD immersed in water. Oxygenation of these initially H-terminated NCD surfaces decreased the fluorescent quenching while having little effect on the adsorption of protein. Imaging single molecules of adsorbed protein deposited on these surfaces at low protein concentrations may indicate spatial heterogeneity in the quenching mechanism.

Acknowledgements

This research was carried out as part of the Advanced Carbon Nanotechnologies Program. Guilhem Ribeill was supported in part by the HHMI RISE program at N.C. State University. Keith Weninger is supported in part by a Career Award at the Scientific Interface from the Burroughs Welcome Fund. The authors thank Drs. Raquel Hernandez and Dennis Brown as well as Amanda Hafer for their aid in the radio-labeling experiments, Franz Koeck for technical assistance, and an anonymous referee for useful suggestions related to these tests.

References

[1] M.I. Landstrass, K.V. Ravi, Appl. Phys. Lett. 55 (1989) 975.
[2] S.R. Gi, K. Tashiro, S. Tanaka, T. Fujisawa, H. Kimura, T. Kurosu, M. Iida, Japanese J. Appl. Phys. 38 (1999) 3492.
[3] J. Ristein, M. Riedel, L. Ley, J. Electrochem. Soc. 151 (2004) E315.

[4] F. Maier, M. Riedel, B. Mantel, J. Ristein, L. Ley, Phys. Rev. Lett. 85 (2000) 3472.
[5] V. Chakrapani, J.C. Angus, A.B. Anderson, S.D. Wolter, B.R. Stoner, G.U. Sumanasekera, Science 318 (2007) 1424.
[6] J.S. Foord, C.H. Lau, M. Hiramatsu, R.B. Jackman, C.E. Nebel, P. Bergonzo, Diamond Relat. Mater. 11 (2002) 856.
[7] A. Campion, A.R. Gallo, C.B. Harris, H.J. Robota, P.M. Whitmore, Chem. Phys. Lett. 73 (1980) 447.
[8] J.R. Lakowicz, Anal. Biochem. 298 (2001) 1.
[9] J.M. Harris, Poly(ethylene glycol) Chemistry: Biotechnical and Biomedical Applications, Plenum Press, 1992.
[10] S.I. Jeon, J.H. Lee, J.D. Andrade, P.G. Degennes, J. Colloid Interface Sci. 142 (1991) 149.
[11] D. Schwendel, R. Dahint, S. Herrwerth, M. Schloerholz, W. Eck, M. Grunze, Langmuir 17 (2001) 5717.
[12] F. Maier, J. Ristein, L. Ley, Phys. Rev. B 64 (2001) 165411.
[13] R.E. Shroder, R.J. Nemanich, J.T. Glass, Phys. Rev. B 41 (1990) 3738.
[14] J. Birrell, J.E. Gerbi, O. Auciello, J.M. Gibson, J. Johnson, J.A. Carlisle, Diamond Relat. Mater. 14 (2005) 86.
[15] A.C. Ferrari, J. Robertson, Phys. Rev. B 64 (2001).
[16] R.J. Nemanich, J.T. Glass, G. Lucovsky, R.E. Shroder, J. Vac. Sci. Technol. A 6 (1988) 1783.
[17] V. Chakrapani, S.C. Eaton, A.B. Anderson, M. Tabib-Azar, J.C. Angus, Electrochem. Solid-State 8 (2005) E4.
[18] J.M. Garguilo, B.A. Davis, M. Buddie, F.A.M. Kock, R.J. Nemanich, Diamond Relat. Mater. 13 (2004) 595.
[19] L. Ostrovskaya, V. Perevertailo, V. Ralchenko, A. Dementjev, O. Loginova, Diamond Relat. Mater. 11 (2002) 845.
[20] K.F. Chong, K.P. Loh, S.R.K. Vedula, C.T. Lim, H. Sternschulte, D. Steinmuller, F.S. Sheu, Y.L. Zhong, Langmuir 23 (2007) 5615.
[21] R.J. Narayan, W. Wei, C. Jin, M. Andara, A. Agarwal, R.A. Gerhardt, C.C. Shih, C.M. Shih, S.J. Lin, Y.Y. Su, R. Ramamurti, R.N. Singh, Diamond Relat. Mater. 15 (2006) 1935.
[22] W. Okroj, M. Kaminska, L. Klimek, W. Szymanski, B. Walkowiak, Diamond Relat. Mater. 15 (2006) 1535.
[23] C. Popov, W. Kulisch, J.P. Reithmaier, T. Dostalova, M. Jelinek, N. Anspach, C. Hammann, Diamond Relat. Mater. 16 (2007) 735.
[24] M. Antia, L.D. Islas, D.A. Boness, G. Baneyx, V. Vogel, Biomaterials 27 (2006) 679.
[25] M. Unger, E. Kartalov, C.S. Chiu, H.A. Lester, S.R. Quake, Biotechniques 27 (1999) 1008.
[26] J. Enderlein, Chem. Phys. 247 (1999) 1.
[27] H. Yokota, K. Saito, T. Yanagida, Phys. Rev. Lett. 80 (1998) 4606.
[28] S. Tunc, M.F. Maitz, G. Steiner, L. Vazquez, M.T. Pham, R. Salzer, Colloid. Surface B 42 (2005) 219.
[29] C.E. Hall, H.S. Slayter, J. Biophys. Biochem. Cytol. 5 (1959) 11.